MICROMECHANICAL MODELING OF PROCESS-INDUCED RESIDUAL STRESSES IN Ti-24Al-11Nb/SCS-6 COMPOSITE

N. Chandra, C.R. Ananth, and H. Garmestani

N. Chandra,[1] *C. R. Ananth,*[1] *and H. Garmestani*[1]

Micromechanical Modeling of Process-Induced Residual Stresses in Ti-24Al-11Nb/SCS-6 Composite

Authorized Reprint 1994 from Journal of Composites Technology & Research, JANUARY 1994

REFERENCE: Chandra, N., Ananth, C. R., and Garmestani, H., **"Micromechanical Modeling of Process-Induced Residual Stresses in Ti-24Al-11Nb/SCS-6 Composite,"** *Journal of Composites Technology & Research*, JCTRER, Vol. 16, No. 1, January 1994, pp. 37–46.

ABSTRACT: A crucial problem in the application of Metallic and Intermetallic Matrix Composites (MMCs and IMCs) is the presence of high levels of residual stresses induced during the fabrication process. This process-induced stress is essentially thermal in nature, and is caused by a significant difference in the coefficients of thermal expansion (CTE) of the fiber and the matrix and the large temperature differential of the cooling process. Residual stresses may lead to the development of matrix cracking, and may also have an adverse effect on the thermomechanical properties of the composites, e.g., stress-strain behavior, fracture toughness, fatigue, and creep. A micromechanical analysis is needed to study the effects of residual stresses, since phenomena like damage are local in nature even though they affect the macro properties. An elastic-plastic finite element analysis is performed to model the thermal stresses induced during fabrication of Ti-24Al-11Nb/SCS-6 unidirectional composite and the effect of these stresses on subsequent transverse loading. The state of residual stress induced in this intermetallic composite is found to be quite different from that in Ti-6Al-4V/SCS-6 metal matrix composite which is extensively discussed in the literature. The influence of fiber-matrix interfacial bonding and fiber arrangement on the thermomechanical behavior of Ti-24Al-11Nb/SCS-6 composite is also studied.

KEYWORDS: residual stress, metal matrix, intermetallic matrix, silicon carbide, finite element analysis, elastic-plastic, interface, transverse tension, fiber arrangement

Metallic and intermetallic matrix composites (MMCs and IMCs) are under rapid development for use in propulsion and structural systems of aerospace vehicles. But a crucial problem in their use is the presence of high levels of residual stresses induced during the fabrication process. Residual stresses are the self-equilibrating internal stresses existing in a free body which has no external constraints acting on its boundary [*1*]. Residual stresses arise from the elastic response of the material to an inhomogeneous distribution of inelastic strains that arise due to plasticity, phase transformation, misfit, thermal expansion, etc. This process-induced residual stress in composites is essentially thermal in nature, and is caused by a significant difference in the coefficients of thermal expansion (CTE) of the fiber and the matrix and the large temperature differential of the cooling process.

When the composite is fabricated at high temperatures both the fiber and the matrix are relatively stress-free and when they are cooled down to room temperature, residual stresses are induced due to thermomechanical mismatch. This problem is more predominant in MMC/IMCs and ceramic matrix composites (CMCs) than in polymeric matrix composites (PMCs), due to the higher processing temperatures and higher stiffness of the matrix in MMC/IMCs and CMCs compared to PMCs. Residual stresses may lead to the development of matrix cracking [*2*], and also may have an adverse effect on the thermomechanical properties of the composites, e.g., stress-strain behavior, fracture toughness, fatigue, and creep. Though it is impossible to eliminate process-induced residual stresses, it is possible to minimize their magnitude through the proper selection of fiber and matrix materials with matching thermal characteristics, optimizing the pressure-time-temperature profile of the fabrication method, introducing a compliant layer between fiber and matrix with intermediate properties (CTE, stiffness, and strength), or by combining some of these options.

The problem of the effect of processing on the thermomechanical behavior of different metal matrix composite systems has attracted the attention of many investigators recently. Micromechanical predictions of residual strains are found to be consistent with the experimental results in the longitudinal (fiber) direction, but not in the transverse direction [*3*]. Transverse test results on Ti-6Al-4V/SCS-6 MMCs by Johnson et al. [*4*] showed the presence of a peculiar "knee" in the transverse stress-strain curve. Further, edge replica studies of interface by the same authors showed fiber-matrix separation leading to the suggestion that weak fiber-matrix interface strength is a possible cause. Studies of Gunawardena et al. [*5*] indicate that the interfacial bond condition has a significant effect on the state of stress in the matrix which in turn dictates matrix ductility. Nimmer [*6*, *7*] also emphasizes the importance of interphase and thermal residual stresses in the transverse mechanical behavior.

Processing Routes of Composites

The composites are fabricated by consolidating fiber mats over matrix available as powder cloth or cast tape. An alternate method is to plasma spray the matrix material onto a rotating drum wound with the reinforcing fiber, to produce a monolayer of fiber and matrix; monolayers are then assembled to a near-net shape by the simultaneous application of temperature and

[1]Department of Mechanical Engineering, FAMU/FSU College of Engineering, Florida A&M University, Florida State University, Tallahassee, FL 32316-2175.

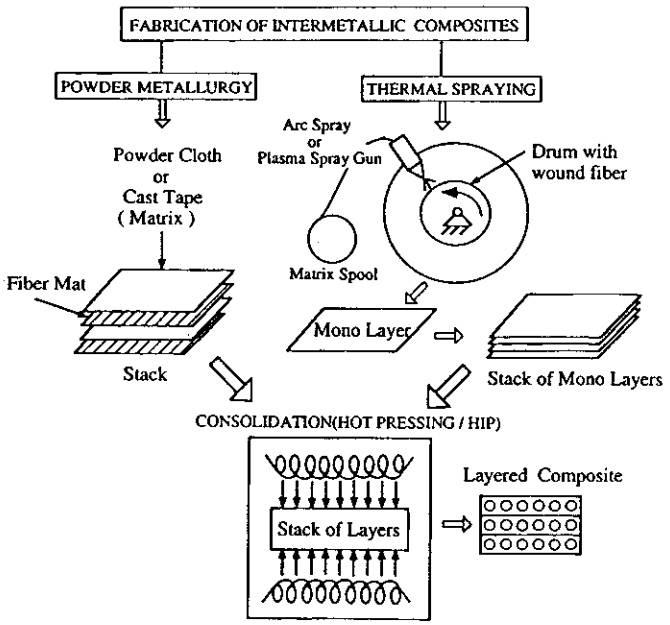

FIG. 1—*Schematic of fabrication process.*

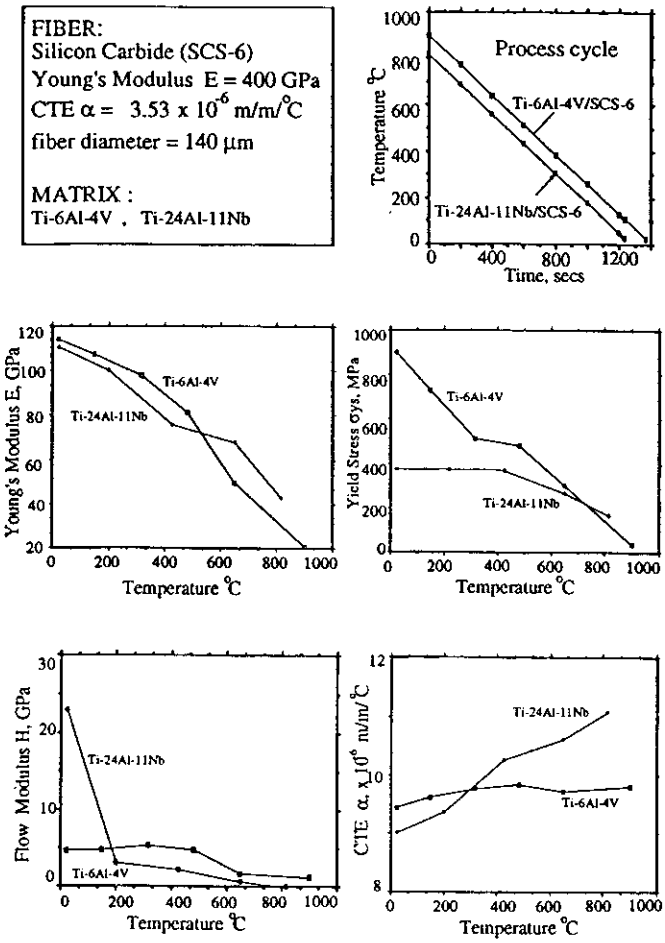

FIG. 2—*Thermomechanical properties and processing cycle.*

pressure over time. A schematic of the fabrication procedures is shown in Fig. 1. The same processing route is adopted for the fabrication of many composite systems including the Ti-6Al-4V/SCS-6 metallic matrix composite and Ti-24Al-11Nb/SCS-6 intermetallic matrix composite which are considered for analysis in this study.

The state of stress at the peak temperature of the fabrication cycle can be assumed to be zero in the matrix and fiber. The consolidated composite is assumed to cool from a temperature of 900°C at a cooling rate of 2300°C/h in the case of MMC [7]. Also, as shown in Fig. 2, the IMC is cooled at the same cooling rate from 815°C [2]. Both the composites are cooled to room temperature. The thermal strain produced then is purely a result of the mismatch of CTE and the magnitude of stress depends on the mechanical stiffness properties. It is to be noted that the thermal and mechanical properties of the constituents, Young's modulus, E, yield strength, σ_{ys}, flow modulus, H, and coefficient of thermal expansion α are all strong functions of temperature. As will be shown later, consideration of the thermal dependence of these properties is very critical in the evaluation of the state of residual stress in this class of composites.

Analytical and Numerical Models

Theoretical analysis for the determination of residual stresses in composites can be considered as an extension of the study of inhomogeneous materials subjected to thermomechanical loading. In many of the analyses, the composites are treated as a class of materials with inhomogeneities or inclusions embedded in a matrix. There is a large literature base available if the materials considered are elastic in nature; however, recently great emphasis has been placed on accounting for the nonlinear behavior of the constituents, especially the matrix. The micromechanics-based analytical models for the above class of problems broadly fall into two categories; namely, elasticity-based solution methods and self-consistent methods.

Elasticity-based solution methods involve solving elastic boundary value problems. Hashin [8] and later Christensen [9] used the elasticity approach to predict the effective elastic properties of the composites. Hashin applied energy principles to arrive at comprehensive bounds for these properties, which are widely used by later researchers for validating their models. Due to the complexity of the equations involved, these models are not easily extendable to inelastic regime.

Self-consistent methods involve volume averaging schemes where the stresses and strains in the matrix and fiber must be in balance with the stresses and strains in a hypothetical smeared or effective material [10]. Most of these models are based on Eshelby's equivalent inclusion method [11] for dilute concentrations. The main advantage of this class of models is that they can be expressed in compact tensor form, and hence easily extendable to inelastic regions. Mori and Tanaka [12] extended the basic Eshelby method to nondilute conditions by considering the inclusion interactions. This method also offers an explicit solution making it suitable for incorporation in numerical schemes. An exhaustive overview of different self-consistent schemes can be found in Ref 13.

Many numerical methods have been employed to determine the processing-induced residual stresses in unidirectional fiber reinforced MMCs and IMCs. Aboudi [14] used his method of cells to predict thermal residual stress in both unidirectional and laminated composites of SCS-6/Ti-15Al-3V system. Later Reddy [15] showed that Aboudi's method is a special case of

finite element method with multiple fibers. Krempl [*16*] used the vanishing fiber diameter model of Dvorak to evaluate residual stress in Boron/Al and Graphite/Al systems. For consideration of inelastic matrix material properties strongly dependent on temperature, and the effects of fiber arrangement, e.g., square, square diagonal, and hexagonal packing, in the determination of residual stresses finite element method (FEM) appears to be an effective computational procedure. Nimmer et al. [*6,7*] and later Robertson et al. [*17*] used FEM to study the fiber/matrix interface effects in Ti-6Al-4V/SCS-6 MMC in the presence of process-induced residual stresses. Wisnom [*18*] modeled the transverse tensile ductility of 6061 Al/SCS-8 MMC using FEM and included the effect of residual stresses induced during processing.

Contents of This Paper

In this paper, FEM is employed to study the origin and the effects of residual microstresses introduced during fabrication processes for two classes of composites, MMC and IMC. Ti-6Al-4V alloy is selected as the model metallic matrix with Titanium Aluminide (Ti-24Al-11Nb) as the intermetallic matrix with a continuous fiber of Silicon Carbide SCS-6. Some of the modeling issues including *the choice of two-dimensional plane field approximations, the effect of nonlinear material (elastic-plastic with strain hardening) behavior at elevated temperatures, the effect of interfacial bonding conditions, thermomechanical behavior of the composite with residual stresses under various service conditions, and the effect of packing geometry* are examined.

It is seen that in the case of IMC, matrix yielding occurs purely from a thermal cooling process; this is different from the MMC systems like Ti-6Al-4V/SCS-6 where the matrix remains in the elastic range throughout the cooling cycle from processing to room temperature. The yielding in IMC introduces concomitant elastic-inelastic regime and affects the stiffness and strength properties. These issues are analyzed in detail.

Finite Element Model

The purpose of the finite element model is to predict the spatial distribution of the state of stress and elastic/inelastic strain in the composite system. The first composite system studied is the MMC, composed of coated silicon carbide fibers in a Ti-6Al-4V matrix. Though this system has been analyzed in detail [*6,7,17*], the results are used in this work for the purposes of validation and form the basis for comparison with IMC.

Representative Volume and Boundary Conditions

A typical representative volume element (RV) of the composite for the case of rectangular packing is shown in Fig. 3. This unit cell can be repeated infinitely to fill the entire volume. Due to symmetry only a quarter of this unit cell needs to be considered for analysis. Figure 3 shows the finite element mesh with the specified boundary conditions. *X*-displacement on the *y*-axis and *y*-displacement on the *x*-axis are kept zero to maintain the symmetry conditions. Since a rectangular unit cell should remain as a rectangle, the edge AB should have the same *x*-displacement, and BC the same *y*-displacement at all times during thermal and mechanical loading. The aspect ratio *R* (*AB/BC*) used is 1.0 (square array) unless specified otherwise. In the case of 3-D

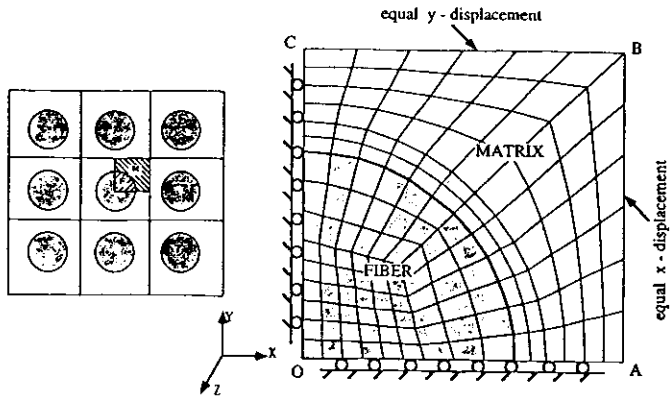

FIG. 3—*Finite element discretization with boundary conditions for a 2-D model.*

model, *x*-displacement on the *yz*-plane through the origin and *y*-displacement on the *xz*-plane through the origin are kept zero. Also, all the nodes in each free surface should undergo the same displacement in the direction normal to the surface. The finite element simulation is performed using MARC nonlinear finite element code in VAX/VMS system.

Modeling the Material Behavior

Preliminary studies indicate that the fiber stresses always remain well below the yield strength. Hence, a linear elastic material model is used for the fiber with temperature independent material properties. The matrix is modeled as an elastic-plastic-strain hardening material with the thermomechanical properties [*2,7*] varying as a function of temperature as shown in Fig. 2. Von Mises yield criterion along with associated flow rule are used in modeling the matrix. Isotropic hardening is assumed.

Two-Dimensional Plane Field Approximations

The problem can be modeled using a full 3-D version, or by making 2-D plane field approximations, which include plane stress, plane strain, or generalized plane strain [*2,6,7,19*]. It is obviously preferable to model the problem using a 2-D version to reduce computational effort without sacrificing accuracy. In this work, 4-noded quadrilateral elements are used in all the 2-D models and 8-noded brick element is used in the 3-D model. Seventy-two elements each are used to model the matrix and the fiber. Internal thermal loads are generated under the assumption that at any given time the temperature is spatially uniform throughout the composite. Preliminary numerical analysis indicates that there may not be a large thermal gradient between the fiber and the matrix for a cooling rate of 2300°C/h.

Comparison of Finite Element Models

Figure 4 shows the axial and equivalent Von Mises stresses when the problem is solved using plane strain, generalized plane strain and 3-D models. The in-plane stresses predicted by all the three models are found to be matching, and hence they are not shown. A plane stress model (not shown in the figure) by definition neglects axial stress which is unacceptable. It can be seen from Fig. 4 that the plane strain model predicts tensile stresses ($\sigma_{zz} > 0$) both in the fiber and matrix, since the thermal contrac-

tion during cooling is prevented by the assumption $\epsilon_{zz} = 0$. However, in the generalized plane strain and 3-D models the entire composite contraction is considered with fiber in compression ($\sigma_{zz} < 0$) and matrix in tension ($\sigma_{zz} > 0$). Generalized plane strain models allow for a nonzero value of ϵ_{zz}, while retaining the 2-D framework. The value of ϵ_{zz} in such a model remains uniform throughout the fiber and matrix. The compressive stress distribution in the fiber is relatively uniform and a single value is shown in the figure. This distribution is essential for the satisfaction of force equilibrium in the axial direction. Consequently, the Von Mises stress in the plane strain model is overpredicted, causing yielding near the interface much earlier than the 3-D model. It is to be noted that the generalized plane strain model matches reasonably closely with the 3-D model. Similar trends have been found by Arnold et al. [2]. Hence, to model the processing of composites generalized plane strain is a minimum requirement and all the analyses presented later in this paper use this approximation with the same level of finite element discretization.

Modeling the Transverse Behavior

The fiber-matrix interface effects play an important role in the modeling of transverse mechanical behavior of MMC and IMC. The assumption of perfect bonding at the fiber-matrix interface sometimes leads to erroneous results since in many systems partial debonding occurs due to thermal, chemical, and mechanical incompatibility. Tests of transverse response and subsequent edge replica studies of Ti-6Al-4V/SCS-6 composites conducted by Highsmith et al. [19] proves the presence of weak interface. In such a case the bond strength is only a percentage of the total perfect bond strength value; however, at present, the prediction of bond strength is heuristic in nature. Assumption of weak or strong interface conditions significantly changes the computed mechanical properties. In this analysis, the case of zero interface bond strength is considered, and hence can serve as a lower bound of transverse stress-strain behavior.

Finite Element Modeling of Interface

The interface is modeled using springs. Let Node 1 be a typical interface node on the fiber with a corresponding Node 2 on the matrix (Fig. 5). Nodes 1 and 2 are connected by a spring with a constant k. Until separation takes place, Nodes 1 and 2 occupy the same location. Let U_R be the relative displacement between Nodes 1 and 2, i.e.,

$$U_R = U_1 - U_2$$

Let the force between Nodes 1 and 2 be given by F_R, which can be written as

$$F_R = F_x\hat{i} + F_y\hat{j} = kU_R$$
$$= U_{Rx}k_x\hat{i} + U_{Ry}k_y\hat{j}$$

Interface Separation Criterion—A criterion based on relative displacement values is considered. The condition for separation in this case is defined as $U_{Ry} > 0$. The initial value of k is taken four orders of magnitude higher than the Young's modulus of the matrix E_m. k is dropped to a low value of $10^{-4}E_m$ once separation occurs.

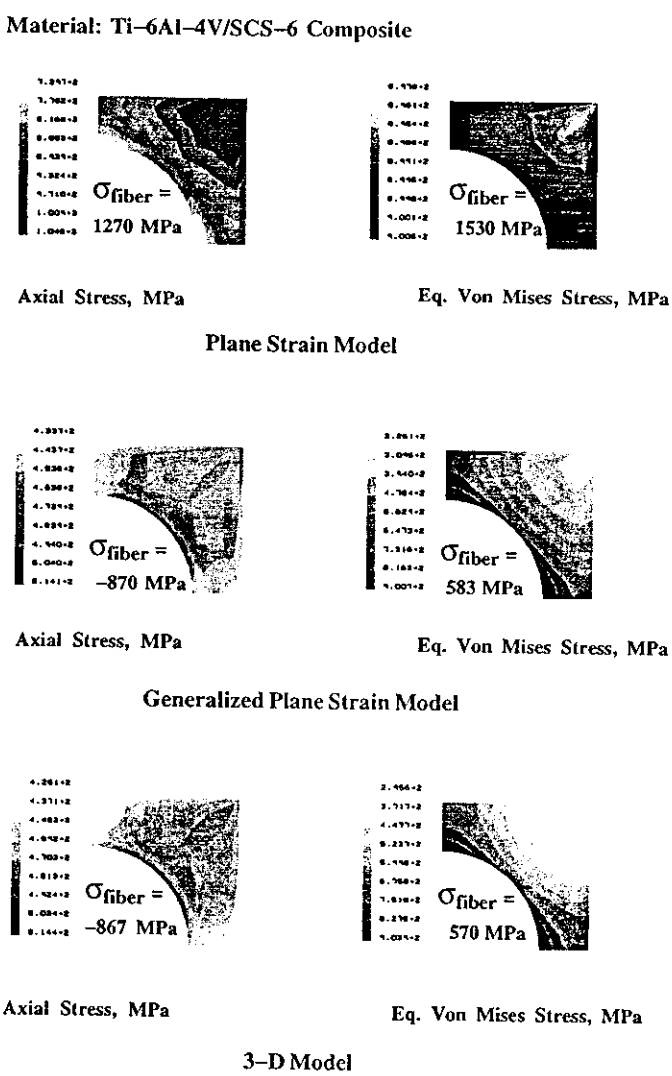

FIG. 4—*Comparison of stress distributions in plane strain, generalized plane strain, and 3-D models.*

Results and Discussions

Residual stress distributions for the Ti-24Al-11Nb/SCS-6 material system are presented in the following section. Volume fraction of fiber considered in this study is 35% unless specified otherwise.

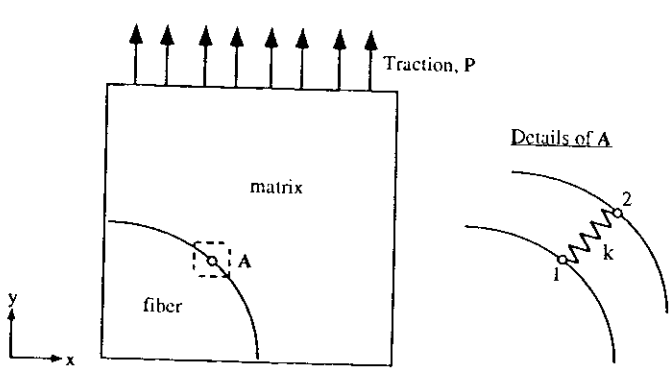

FIG. 5—*Weak interface model.*

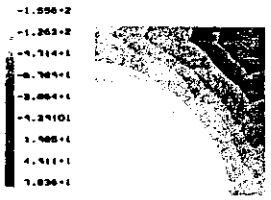

Radial Stress, MPa

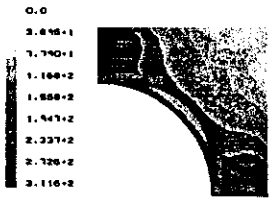

Tangential Stress, MPa

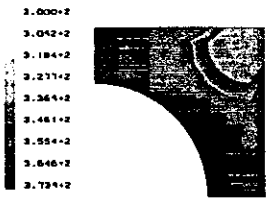

Equivalent VonMises Stress, MPa

FIG. 6—*Residual stress distributions in the matrix of Ti-24Al-11Nb/SCS-6 composite.*

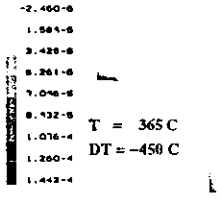

Eq. plastic strain

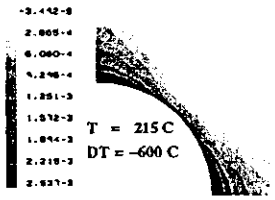

Eq. plastic strain

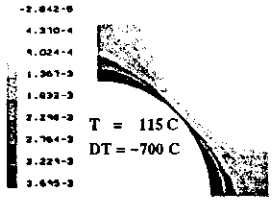

Eq. plastic strain

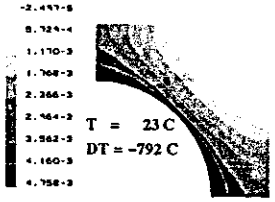

Eq. plastic strain

FIG. 7—*Variation of equivalent plastic strain with temperature in the matrix of Ti-24-Al-11Nb/SCS-6 composite.*

Residual Stresses in Ti-24Al-11Nb/SCS-6 Composite

Figure 6 shows the radial, tangential, and Von Mises stresses present in the matrix of Titanium Aluminide composite at the end of the processing cycle. Though the CTE mismatch of the two systems (Ti-24Al-11Nb/SCS-6(IMC), Ti-6Al-4V/SCS-6(MMC)) are approximately same, the mechanical properties of the matrix in IMC (especially σ_{ys}) are significantly lower than that of matrix in MMC as shown in Fig. 2. Von Mises stress profile shows that a significant portion of the matrix has already yielded just by cooling from the processing temperature. This introduces additional factors like redistribution of stresses, propagation of inelastic strains etc., which have to be analyzed thoroughly making it necessary to track down these quantities as a function of decreasing temperature. This makes the analysis of the IMC system under study more complex than the model MMC system chosen which remains elastic all through the cooling process.

When the composite is cooled from the processing temperature, residual stresses build up and accumulate till room temperature is reached. This is essentially from $(\alpha_{matrix} - \alpha_{fiber})\Delta T$ effect. If during the process of cooling, the Von Mises stress exceeds yield stress at any temperature at a given point (x, y), then yielding occurs. The point (x, y) is in elastic or plastic range in the next increment of time depending on the magnitude of the incremental stress and the change in yield stress value. If the increase in yield stress with temperature $\frac{\Delta\sigma_{ys}}{\Delta T}$ is larger than $\frac{\Delta\sigma(x,y)}{\Delta T}$ in that region, then the stress remains in elastic range. However, if $\frac{\Delta\sigma_{ys}}{\Delta T}$ is less than $\frac{\Delta\sigma(x,y)}{\Delta T}$, then further yielding takes place at (x, y). Since the stress at (x, y) cannot increase more than σ_{ys}, the yield zone grows radially outwards to satisfy the force equilibrium conditions. This is evidenced by the propagation of plastic strain shown in Fig. 7. In the material system under consideration (IMC), $\Delta\sigma_{ys} \simeq 0$ (i.e., $\sigma_{ys} \simeq 370$ MPa) below 400°C (Fig. 2), thus the yield zone propagates well into the matrix with further decrease in temperature.

It is found that the in-plane stresses are maximum along the direction where the neighboring fibers are at the closest distance (namely, x or y axes for the case of rectangular array of packing) wheras the axial stress has its maximum along the diagonal. The Von Mises equivalent stress has its peak at the fiber-matrix interface (along x or y-axes), and hence the first yield occurs in this region (denoted by R in Fig. 8) at around 365°C when the composite is cooled from the processing temperature of about 815°C. This is also further confirmed from Fig. 7 showing the initiation of plastic strain at that temperature. The point R remains yielded when cooled down to room temperature; when the composite is subsequently heated to the service temperature, the point R goes into the elastic range due to elastic unloading caused by pure thermal loads (see Fig. 8).

High tensile stresses cause cracks to propagate in a material, tangential stress resulting in radial cracks and axial stress causing in-plane cracks, in a plane normal to the fiber in the present study. Hence, it becomes necessary to track the components of stresses in the matrix which are tensile so that the magnitude and the region of occurrence of maximum tensile stresses can be analyzed. As seen from Fig. 8, processing causes axial and circumferential stresses to be tensile in nature. The circumferential (tangential) stress has the highest magnitude and can be the primary source for radial cracks; in fact, radial cracks have been observed in the fiber-matrix interface [*3*]. As the material is heated back, tangential stress continues to reduce and in fact becomes compressive above 450°C, when radial stress becomes tensile. Another interesting observation is the region of occurrence of the maximum tensile stresses. Figure 9 shows the spatial distribution of tangential stress as cooling progresses. When the temperature is 365°C, the distribution is radially symmetric and the stress field is fully elastic. As cooling continues, yielding occurs at the interface along the x-axis (and y-axis) and the yield zone moves outward radially. Figure 10 shows the tangential

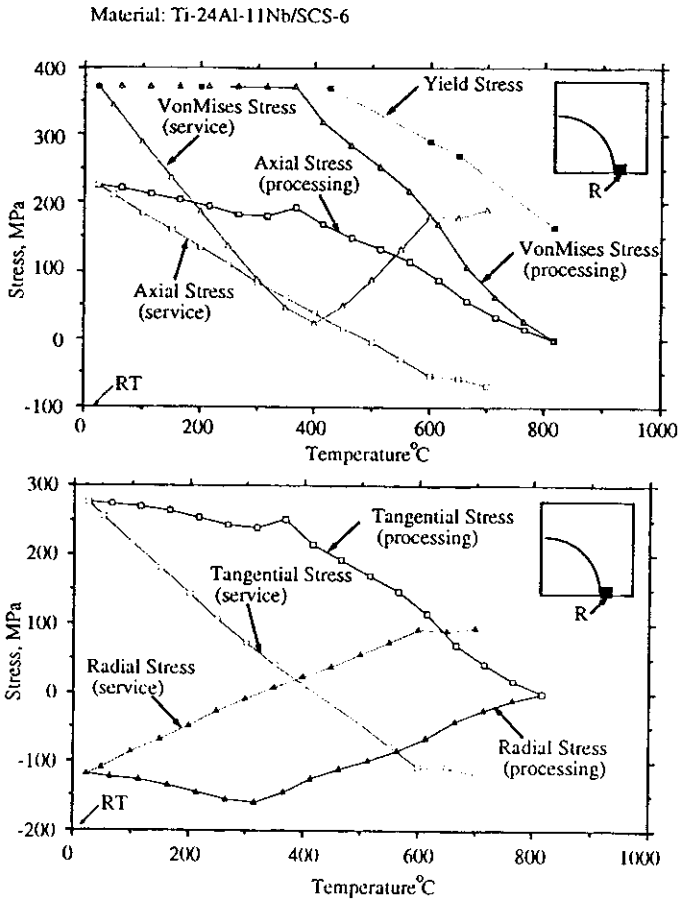

FIG. 8—*Variation of residual stress components at R during processing and in service.*

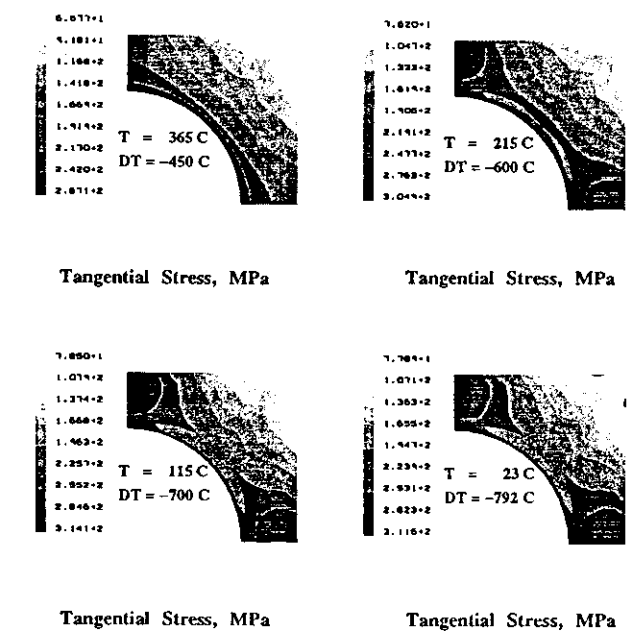

FIG. 9—*Variation of tangential stress with temperature in the matrix of Ti-24Al-11Nb/SCS-6 composite.*

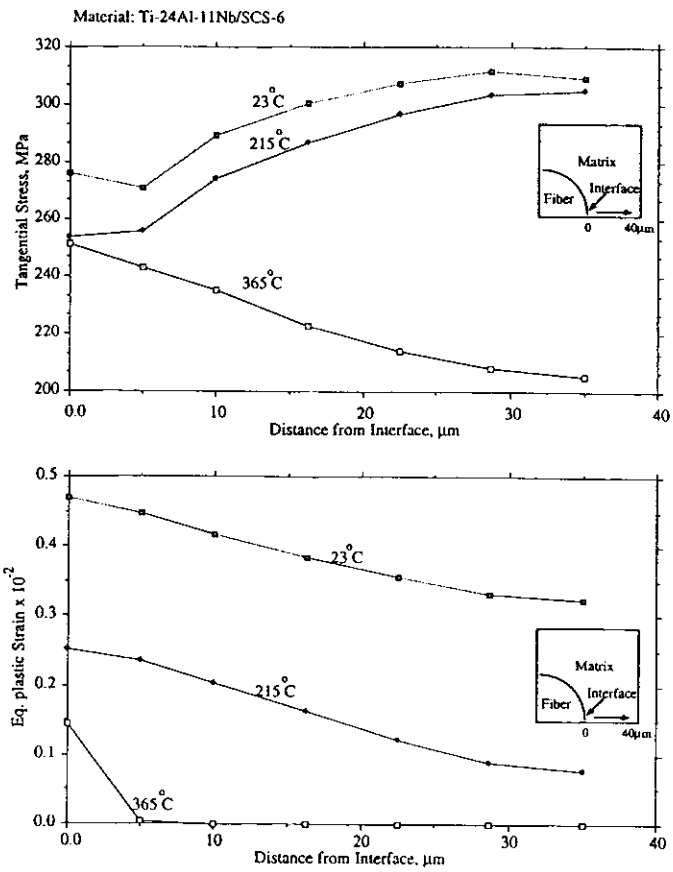

FIG. 10—*Variation of tangential residual stress and residual plastic strain along the axis of symmetry.*

stress along x-axis at 365°C, 215°C, and at room temperature. The location of maximum tangential stress moves away from the interface. This can be attributed to the redistribution of stresses with increase in plastic strain.

Comparison with Experimental Results

Wright et al. [*3*] carried out residual stress measurements in IMC systems using Neutron Diffraction (ND) and X-ray Diffraction methods. These techniques are limited to measuring the average value of strain depending on the spot size of X-ray and Neutron beams. Table 1 compares the finite element predictions of process-induced residual strains in Ti-24Al-11Nb/SCS-6 composite with the experimental results. It can be seen that the measured values of strains in the matrix match quite well with the computed values in the longitudinal direction. However, in the transverse direction, the values are not consistent but all the

TABLE 1—*Average residual strain comparison at room temperature in the matrix of Ti-24Al-11Nb/SCS-6 composite.*

Strain	FEM[a]	XRD[b]	ND[c]
Longitudinal	0.00347	0.00320	0.00370
Transverse	−0.00061	0.00120	−0.00020

[a]Finite Element Method.
[b]X-ray Diffraction Technique.
[c]Neutron Diffraction Technique.

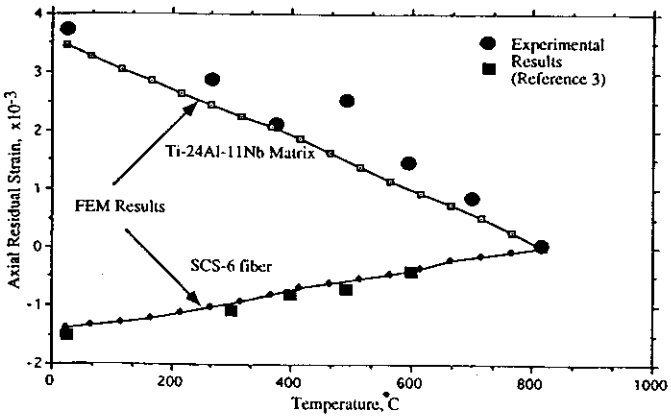

FIG. 11—*Experimental comparisons.*

values are extremely low. Figure 11 shows close correlation between the measured and computed values of longitudinal strains in the matrix and fiber regions as the composite is cooled from the processing temperature. In the above comparisons, the FEM results are the computed averages over the matrix and fiber domains. This is obtained by multiplying the elemental averages

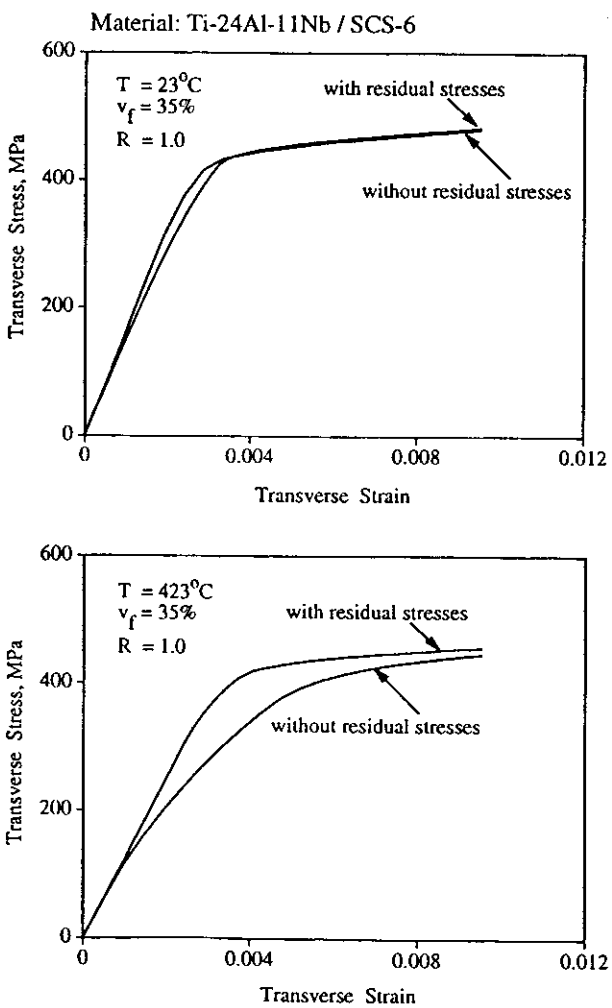

FIG. 12—*Effect of residual stress on transverse tensile response with perfect bonding at the interface.*

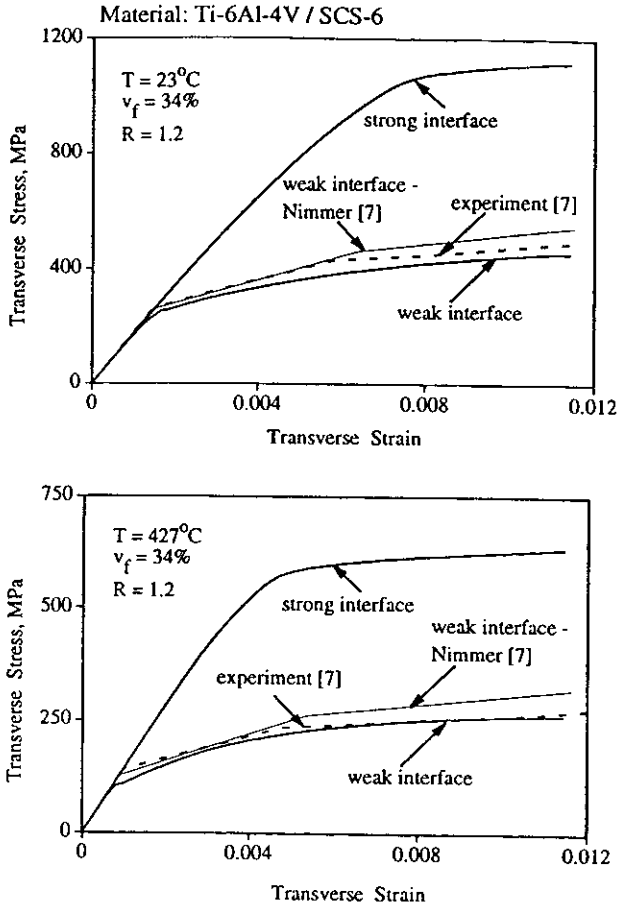

FIG. 13—*Transverse tensile response of strong and weak interface Ti-6Al-4V/SCS-6 composite with residual stresses.*

by the corresponding element area (2-D)/volume (3-D) fractions and adding them up. The elemental average is obtained by multiplying the Gauss point quantities by corresponding weighting functions and dividing the cumulative value by the area of that element.

Effect of Residual Stress on Transverse Response

Mechanical response of the composites at room temperature and elevated temperatures is a prime factor in the design of composites. Since the transverse behavior of the composite becomes critical in many applications, the influence of residual stress on subsequent mechanical loading in the transverse direction has to be analyzed.

Case of Perfect Bonding at the Interface—Figure 12 shows the effect of residual stress on the transverse tensile behavior of the composite at RT and at an operating temperature of 423°C. In this analysis, perfect bonding conditions between the matrix and the fiber is assumed. It is interesting to note that at both the temperatures the transverse load carrying capacity of the composite increases when residual stresses are present, the effect being more predominant at higher temperatures. This can be attributed to the presence of compressive radial stresses at the interface, which delay the onset of yielding, when subjected to transverse tensile load. In all the cases there is a knee in the curve indicating that matrix yielding has initiated.

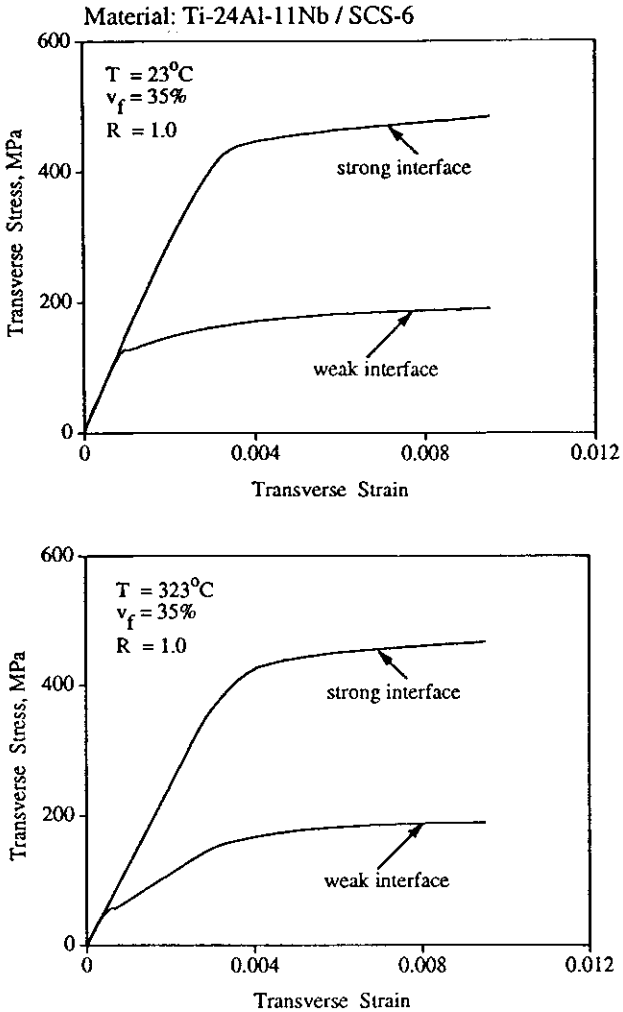

FIG. 14—*Transverse tensile response of strong and weak interface Ti-24Al-11Nb/SCS-6 composite with residual stresses.*

Case of Weak Fiber-Matrix Interface—Figure 13 shows the results of finite element analysis in the cases of perfect bonding and zero interface strength conditions of Ti-6Al-4V/SCS-6 composite at two different temperatures, and compares with the experimental results published by Nimmer [7]. A volume fraction of 34% and an aspect ratio of 1.2 is used to simulate the experimental conditions. Also seen in Fig. 13 are the numerical results of Nimmer which are based on a 3-D contact surface formulation. In Nimmer's model, tensile stresses normal to the interface are not allowed, and shear forces tangential to the interface are transmitted from fiber to matrix according to the law of Coulomb friction. It can be seen that the overall response predicted by the present model, which assumes zero interface strength, compares reasonably well with the experimental results of Nimmer, confirming that the Ti-6Al-4V/SCS-6 system has a very weak interface. The initial separation stress is slightly lower than that of Nimmer's weak interface model, which gives results closer to the experimental values. This may be due to the difference in the separation criteria. The above results suggest that the present model can be used to predict a lower bound of transverse stress-strain behavior of any other unidirectional continuous fiber-reinforced MMC or IMC system.

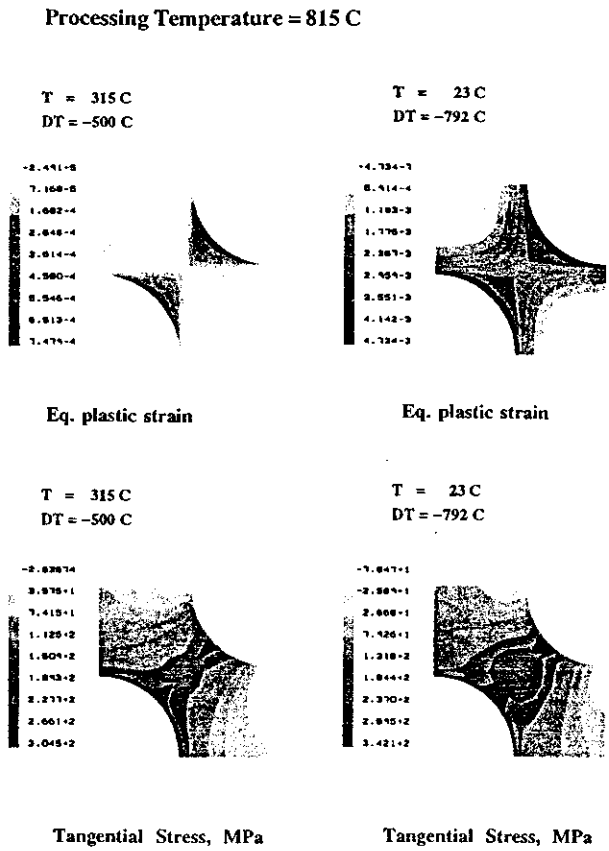

FIG. 15—*Variation of equivalent plastic strain and tangential stress with temperature in the matrix of Ti-24Al-11Nb/SCS-6 composite.*

Figure 14 shows similar results of Ti-24Al-11Nb/SCC-6 composite. It can be seen that the compressive residual stresses at the interface postpone the fiber-matrix debonding, but still the separation occurs well before yielding, causing two distinctive knees in the transverse stress-strain response. The strength of this composite is considerably lower than that of the Ti-6Al-4V/SCS-6 system.

Effect of Fiber Arrangement

The influence of arrangement of fiber in the matrix on residual stresses and subsequent transverse response is analyzed in this section. The arrangements under consideration are regular rectangular and square diagonal arrays. It has been shown by Brokenbrough et al. [20] that square and square diagonal arrays form the bounds in the mechanical response and hexagonal close packed array represents an intermediate value.

As can be seen from Fig. 15 (showing the propagation of plastic strains during processing), the first yield occurs along the diagonal at the fiber-matrix surface for square-diagonal packing. The maximum tangential stress also occurs along the diagonal increasing the cracking tendencies in this plane. The transverse response comparisons (Fig. 16) show that the square-diagonal packing yields at a lower load compared to regular rectangular packing. Perfect bonding conditions are assumed in this analysis.

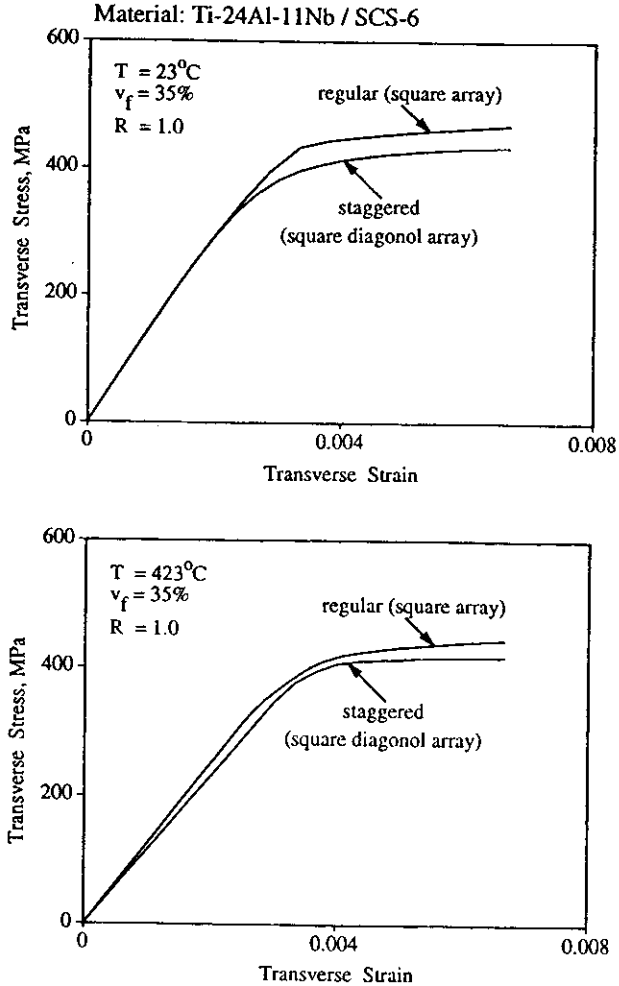

FIG. 16—*Comparison of transverse tensile response of square array and square diagonal array.*

Summary and Conclusions

FEM is used to study the origin of residual stresses in two classes of composites, metal matrix composite Ti-6Al-4V/SCS-6 and intermetallic matrix composite Ti-24Al-11Nb/SCS-6. From the various plane field approximations it is concluded that generalized plane strain is a minimum requirement to model the composite consolidation process properly. While the processing conditions of these two composites are similar and so are the thermal properties of their matrices, a different distribution of residual stress is obtained in Ti-24Al-11Nb/SCS-6. This is due to the fact that matrix yielding occurs during the cooling process thereby introducing inelastic strains. This produces a redistribution of stresses during subsequent cooling, increasing the region of higher stresses in the composite. This result is different compared to a state of elastic strain in Ti-6Al-4V/SCS-6 composite where high value of stresses occur only near the fiber-matrix interface. Residual stresses are relieved when the Ti-24Al-11Nb/SCS-6 is heated back to operating temperature. Transverse stress-strain behavior of the composite is influenced by the presence of residual stresses and the influence is stronger at service temperature compared to that at room temperature; the interface conditions also affect the transverse response. It is found that stress distribution, the magnitude and location of maximum stress, changes with fiber arrangement. It also affects the transverse stress-strain response.

Acknowledgments

The authors wish to acknowledge the National Science Foundation (RIMI) and NASA for providing partial financial assistance in support of this project.

References

[1] Mura, T., *Micromechanics of Defects in Solids*, Martnus Nijhoff Publishers, The Hague, Netherlands, 1982.

[2] Arnold, S. M., Ayra. V. K., and Melis, M. E., "Elastic/Plastic Analyses of Advanced Composites Investigating the Use of the Compliant Layer Concept in Reducing Residual Stresses Resulting from Processing," *NASA TM 103204*, 1990.

[3] Wright, P. K., Kupperman, D., Wadley, H., "Thermal Stress Effects in Intermetallic Matrix Composites," *NASA Report CP 10082*.

[4] Johnson, W. S., Lubowinski, S. J., and Highsmith, A. L., "Mechanical Characterization of Unnotched SCS-6/Ti-15-3 Metal Matrix Composites at Room Temperature," in *Thermal and Mechanical Behavior of Metal Matrix and Ceramic Matrix Composites, ASTM STP 1080*, J. M. Kennedy, H. H. Moeller, and W. S. Johnson, Eds., American Society for Testing and Materials, Philadelphia, 1990, pp. 193–218.

[5] Guanwardena, R. S., Jansson, S., Leckie, F. A., "Transverse Ductility of Metal Matrix Composites," *Failure Mechanisms in High Temperature Composite Materials*, AMD-Vol. 122, ASME Publications, 1991, pp. 23–30.

[6] Nimmer, R. P., "Fiber-Matrix Interface Effects in the Presence of Thermally Induced Residual Stresses," *Journal of Composites Technology and Research*, Vol. 12, No. 2, 1990, pp. 65–75.

[7] Nimmer, R. P., Bankert, R. J., Russel, E. S., et al., "Micromechanical Modeling of Fiber-Matrix Interface Effects in Transversely Loaded SiC/Ti-6-4 Metal Matrix Composites," *Journal of Composites Technology and Research*, Vol. 13, No. 1, Spring 1991, pp. 3–13.

[8] Hashin, Z., "Analysis of Properties of Fiber Composites with Anisotropic Constituents," *Journal of Applied Mechanics*, Vol. 46, 1979, pp. 543–550.

[9] Christensen, R. M. and Lo, K. H., "Solutions for Effective Properties in Three Phase Sphere and Cylinder Models," *Journal of the Mechanics and Physics of Solids*, Vol. 27, 1979, pp. 315–329.

[10] Gramoll, K. C., Walker, K. P., Freed, A. D., "Investigation of Effective Material Properties for Viscoplastic Fibrous Composites Using the Self-Consistent and Mori-Tanaka Methods," *High Temperature Constitutive Modeling—Theory and Application*, AMD-Vol. 121, ASME Publications, 1991, pp. 439–449.

[11] Eshelby, J. D., "The Determination of the Elastic Field of an Ellipsoidal Inclusion and Related Problems," *Proceedings of Royal Society of London, Ser. A*, Vol. 241, 1957, pp. 376–396.

[12] Mori, T. and Tanaka, K., "Average Stress in Matrix and Average Elastic Energy of Materials with Misfitting Inclusions," *Acta Metallurgica*, Vol. 21, 1973, pp. 571–574.

[13] Gramoll, K. C., Walker, K. P., Freed, A. D., "An Overview of Self-Consistent Methods for Fiber Reinforced Composites," *NASA TM 103713*, 1991.

[14] Aboudi, J., "Micromechanical Analysis of Composites by the Method of Cells," *Applied Mechanics Reviews*, Vol. 42, No. 7, 1989, pp. 193–221.

[15] Reddy, J. N. and Teply, J. L., "A Unified Formulation of Micromechanics Models of Fiber-Reinforced Composites," *Inelastic Deformation of Composite Materials, Proceedings of IUTAM Symposium*, Troy, NY, G. J. Dvorak, Ed., 1990, pp. 341–370.

[16] Krempl, E. and Yeh, N. M., "Residual Stresses in Fibrous Metal Matrix Composites: A Thermoviscoplastic Analysis," *Inelastic Deformation of Composite Materials, Proceedings of IUTAM Symposium*, Troy, NY, G. J. Dvorak, Ed., 1990, pp. 411–444.

[17] Robertson, D. D. and Mall, S., "Fiber-Matrix Interface Effects upon Transverse Behavior in Metal-Matrix Composites," *Journal of Composites Technology and Research*, Vol. 14, No. 1, Spring 1992, pp. 3–11.

[18] Wisnom, M. R., "Micromechanical Modelling of the Transverse Tensile Ductility of Unidirectional Silicon Carbide/6061 Aluminum," *Journal of Composites Technology and Research*, Vol. 14, No. 2, Summer 1992, pp. 61–69.

[19] Highsmith, A. L., Shin, D., and Naik, R. A., "Local Stresses in Metal Matrix Composites Subjected to Thermal and Mechanical Loading," *Thermal and Mechanical Behavior of Metal Matrix and Ceramic Matrix Composites, ASTM STP 1080*, J. M. Kennedy, H. H. Moeller, and W. S. Johnson, Eds., American Society for Testing and Materials, Philadelphia, 1990, pp. 3–19.

[20] Brokenbrough, J. R., Suresh, S., and Wienecke, H. A., "Deformation of Metal-Matrix Composites with Continuous Fibers: Geometrical Effects of Fiber Distribution and Shape," *Acta Matallurgica Materiala*, Vol. 39, No. 5, 1991, pp. 735–752.